White-light emission of ZnO nanoparticles prepared by sol–gel method*

Li Shi-Shuai(李世帅), Zhang Zhong(张 仲)†, Hang Jin-Zhao(黄金昭), Feng Xiu-Peng(冯秀鹏), and Liu Ru-Xi(刘如喜)

School of Physical Science, University of Jinan, Jinan 250022*, China*

(Received 22 April 2011; revised manuscript received 26 June 2011)

In:ZnO nanoparticles are prepared by the sol–gel process. The ratios of In/(Zn+In) are 0%, 5%, 8%, 10%, and 15%, respectively. Crystal phase structures and optoelectronic properties of these samples are characterized and the chromaticity coordinates of different samples are also calculated in CIE–XYZ colour system. The results show that preferred growth direction of ZnO changes from (002) plane to (001) plane and interplanar distance becomes shorter. When the doping amount of In is 5%, Zn atoms are completely replaced by In atoms. The resistivities of the samples first decrease, then increase afterwards with the increase of the amount of In. With the increase of In, the ultraviolet emission is redshifted and new peaks occur at 465 nm, 535 nm, and 630 nm. The sample with 10% indium has white-light emission. The band structures of samples with 0% and 12.5% indium are investigated by the first principle method. The mechanism of white emission is discussed from the viewpoint of additional energy levels.

Keywords: sol–gel resistivity, chromaticity coordinate white-light emitting, first principle

PACS: 71.55.Gs, 73.61.Ga, 78.66.Hf **DOI:** 10.1088/1674-1056/20/12/127102

1. Introduction

ZnO as a luminescent material, has the advantage of blue, blue–green and ultraviolet light emission.[1−3] The emission of pure ZnO is mainly ultraviolet and yellow–green. Experimental results showed that the emission of ZnO was dominated by preparation methods and conditions, post-processing, and so on.[4,5] ZnO materials prepared under different conditions can have different level structures. So far, the study of white light emission of ZnO is still in its infancy. ZnO nanocrystals were prepared using chemical precipitation by Lu *et al.*[6] (2002), who found that the sample emitted white light with high-energy excitation. In 2005, Hao[7] developed a white light emitting diode using ZnO nanowires, but the emission was unstable. ZnO nanotubes with white light emission were prepared by Guo *et al.*[8] (2009). In their study, the ZnO samples were synthesized using a two-step method, which means this preparation is complex. In the same year, Lin and Lee[9] prepared the ZnO nanopillar on a blue organic light-emitting thin film by hydrothermal method successfully, and they found that the nanopillar emitted white light. However, this method requires very strict conditions, as in their study a low temperature hydrated solution and P type blue-ray organic material as a substrate are needed.

Until now, reports on white emission with doped ZnO has been rare. Doped ZnO can form more energy levels than undoped ZnO, so that the spectra become more diverse.[10−12] Therefore, the white light emission of ZnO could be achieved by the doping method. On the one hand, the radii of In^{3+} (0.081 nm) and Zn^{2+} (0.074 nm) are very close, so the lattice distortion can be avoided in indium-doped Zn; on the other hand, the energy level of the indium atom is richer than that of zinc atom, so the study on white light emission of In-doped ZnO is feasible. In this paper, In:ZnO nanoparticles are prepared by the sol–gel method and the ratios of In:(Zn+In) are 0%, 5%, 8%, 10%, and 15%, respectively. Its crystal structure, optical properties, and luminescence mechanism are studied. The white emission of the sample is investigated in depth, which has potential applications in

*Project supported by the Natural Science Foundation of Shandong Province of China (Grant No. Y2007G14), the Science and Technology Development Projects of Shandong Province of China (Grant Nos. 2009GG2003028 and 2010G0020423), the Doctoral Foundation of University of Jinan, China (Grant No. XBS0845), the Key Laboratory of Luminescence and Optical Information, Ministry of Education, Beijing Jiaotong University, China (Grant No. 2010L0101), and the Scientific Research Foundation of University of Jinan, China (Grant No. XKY1029).

†Corresponding author. E-mail: ss_zhangz@ujn.edu.cn

© 2011 Chinese Physical Society and IOP Publishing Ltd

white-light nanodevices, such as light-emitting diodes and flat panel displays.

2. Experiment

The precursor was prepared by dissolving 0.02-mol zinc acetate and $InCl_3{\cdot}4H_2O$ in deionized water to form a solution ($[Zn^{2+}]$=0.05 ml/L). ZnO nanoparticles were doped with 5%, 8%, 10%, and 15% indium that we want to prepare separately, so the $InCl_3{\cdot}4H_2O$ with the quantities of 0.3086 g, 0.5102 g, 0.6516 g, and 1.0350 g must be needed as indicated by calculation. The $InCl_3{\cdot}4H_2O$ and zinc acetate were mixed together by magnetic stirring for 1 min, then 1.92-ml diethanolamine ($C_4H_{11}NO_2$) was added to the solution and kept at 800 °C in a water-bath on a magnetic stirrer for 5 h. Thus the white gel was made. The gel was moved into a crucible, and then the temperature of the crucible was raised to 80 °C and held constant for 4 h in a furnace. The purpose of annealing is to thoroughly remove impurities in the gel composition. Finally the products were taken out and grinded, and the In-doped ZnO nanoparticles were made. We denote the samples of 0%, 5%, 8%, 10%, and 15% as samples a, b, c, d, and e, respectively.

D8 ADVANCE X-ray diffraction (XRD) was used to characterize the structure of the sample under the following conditions: the radiation source was CuK radiation at a wavelength of 0.154505 nm, scanning ranged from $2\theta = 10°$ to $2\theta = 90°$ at a scanning speed of 8°/min, work voltage was 80 kV and current was 10 mA. A SB120 four-probe test board, SB118 precise DC source and PZ158A DC digital voltage meter were combined to establish a test system to measure the resistivities of the samples. The PL (photoluminescence) spectrum was measured using FS920 fluorescence spectrometer, and the excitation wavelength was 325 nm. All experiments were carried out at room temperature. The first-principles full potential linearized augmented plane wave method (FP-LAPW) was used for studying the band of In-doped ZnO.

3. Results and discussion

The X-ray diffraction analyses of the samples were given in Fig. 1. The results indicate that sample a is zincite in structure contraposing the JCPDS card 36–1451. The intensity of the diffraction peak at (101) decreases with increasing doping ratio. From the above analysis, we can see that the majority of indium atoms entered the crystal lattice of ZnO. In addition, for each crystal sample its FWHM (face diffraction peak width at half maximum) was very small, indicating that the surface of the sample in each crystal is an orderly crystalline. There were no impurity peaks in sample b, indicating that In atoms completely replace Zn atoms for the whole bulk material. There were impure peaks (A, B, C, D, E) in samples c, d, and e.

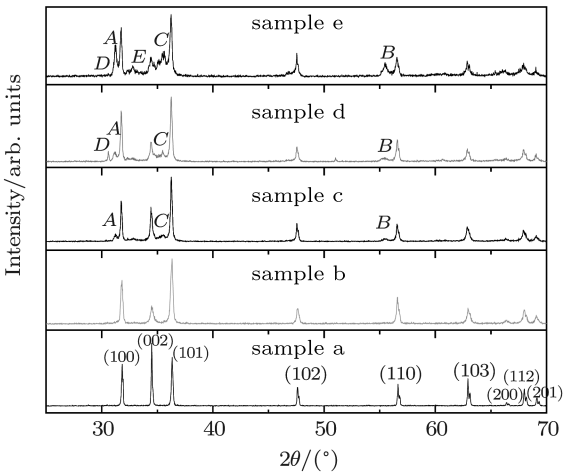


Fig. 1. XRD pattern of In-doped ZnO with different ratios.

By the software (MDI Jide 5.0) we know that these impure peaks formed by the synthesis of In_2O_3 compared with the JCPDS card (22–0336, 65–3170, 06–0416). This phenomenon is due to the fact that more and more indium atoms separated out and combined to form In_2O_3 with oxygen through the increase in the amount of indium doping. Compared with the peaks of sample a, the peaks of samples b, c, d, and e slightly shift toward the high angle direction. From the Bragg equation ($2d\sin\theta = \lambda$, where d is interplanar crystal spacing, θ is the diffraction angle, λ is X-ray wavelength of 0.154 nm) we can see that the interplanar crystal spacing becomes shorter with an increase in the ratio of In/(In+Zn). The change of spacing was due to the fact that the radius of In^{3+} (0.081 nm) was slightly larger than Zn^{2+} (0.074 nm). It is also confirmed that majority of indium atoms entered into the crystal lattice of ZnO.

The samples sheets were prepared by 0.2-g ZnO nanoparticles by dropping the right amount of alcohol. Then the sheets of ZnO were moved into the furnace. The temperature of the sheets was raised to high temperature and held constant for 4 h in the furnace. Their densities increased, which does not affect our analysis, for we only consider the relative change in

resistivity. Figure 3 shows the geometry of the probe configuration.

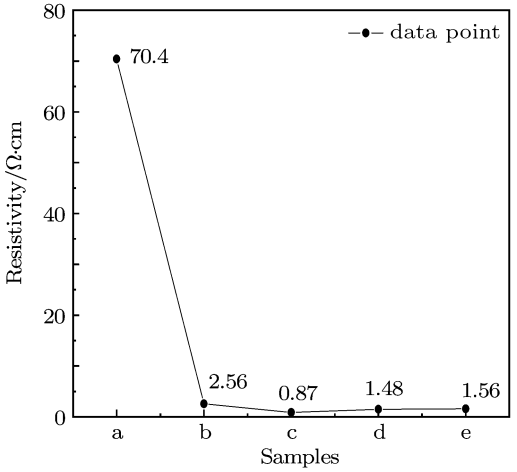


Fig. 2. Resistivities of ZnO nanoparticles with different doping concentrations.

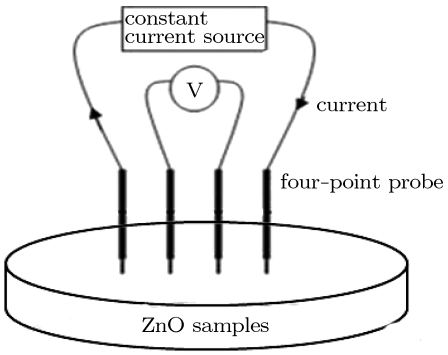


Fig. 3. Geometry of the probe configuration.

A sheet is positioned on the stage of four-probe, so that its current and voltage can be measured. Then we calculate the sample resistivity, according to the following formula:[13,14]

$$\rho = 2\pi \mathrm{S}V/I, \tag{1}$$

where ρ is the resistivity, S (0.2 cm) is the distance between the two probes, V is the voltage, and I is the current. The resistivities are given in Fig. 2. We can see that for In-doped ZnO, the resistivity decreases rapidly. Having a wide band gap, pure stoichiometric ZnO is insulator, but the samples prepared by the experiment inevitably have some defects. The defects can generate free carriers, so the undoped-ZnO nanoparticles can be conductive.[15,16] The radius of In^{3+} is slightly larger than that of Zn^{2+}. Therefore the lattice energy of O^{2-}–In^{3+} is stronger than that of O^{2-}–Zn^{2+}. So In_i (interstitial atom of indium) is easier to form than Zn_i (interstitial atom of Zinc), which can produce more electrons. Furthermore, the valence of indium is higher than that of Zn. In order to maintain charge balance, the oxygen atoms make a slight deviation from their original place, producing a lot of V_O's (oxygen vacancies) in theory. These two electrons occupied by O are weakly bounded around the vacancy. These two electrons easily overcome this restraint and move freely in the crystal, becoming carriers. In this way the resistivity of doped-ZnO is more greatly reduced than that of the intrinsic ZnO. We can also see that the resistivity of the sample first decreases and then increases, with the ratio of In/(In+Zn) increasing. Because of the ionization of In, a Coulomb potential field is generated around the ions. The carriers will be scattered by the Coulomb potential field. The Coulomb potential field increases with the increase of the concentration of doped In, which enhances the scattering of the carriers and reduces the carriers in a special direction.

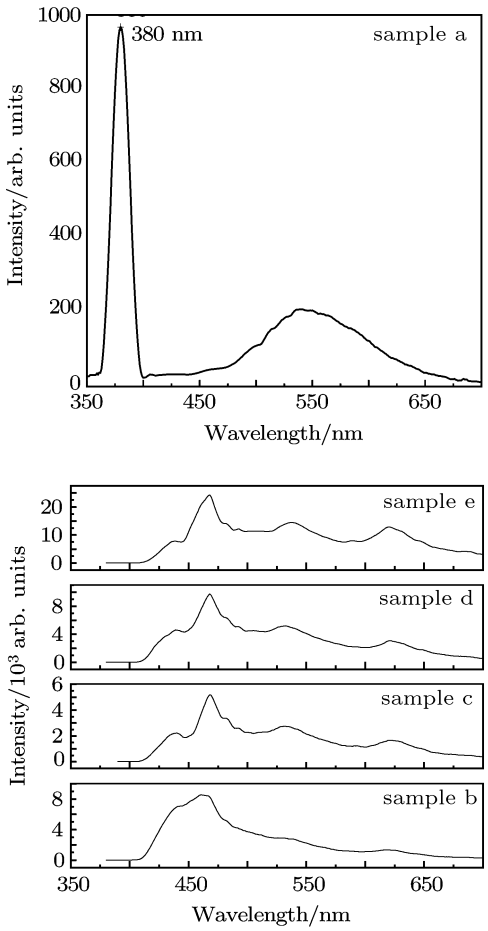


Fig. 4. Photoluminescences of samples a, b, c, d, and e at room temperature.

According to the spectra in Fig. 4, we calculate the chromaticity coordinates of samples a, b, c, d, and

e using the following formula:

$$\left.\begin{aligned} X &= \int_{380}^{780} \mathrm{p}(\lambda)\bar{x}(\lambda)\mathrm{d}\lambda \\ Y &= \int_{380}^{780} \mathrm{p}(\lambda)\bar{y}(\lambda)\mathrm{d}\lambda \\ Z &= \int_{380}^{780} \mathrm{p}(\lambda)\bar{z}(\lambda)\mathrm{d}\lambda \end{aligned}\right\}, \tag{2}$$

$$\left.\begin{aligned} x &= \frac{X}{X+Y+Z} \\ y &= \frac{Y}{X+Y+Z} \end{aligned}\right\}, \tag{3}$$

where $\bar{x}$, $\bar{y}$, $\bar{z}$ are the standard spectral tristimulus values of CIE-1931, $p(\lambda)$ is the spectral intensity distribution, and (x, y) are the chromaticity coordinates. We can calculate the chromaticity coordinates as follows: a (0.36, 0.50), b (0.20, 0.20), c (0.26, 0.31), d (0.30, 0.33), and e (0.25, 0.30). Figure 5 shows the spectral chromaticity coordinates of the samples. (0.30, 0.33) is in the white light area of the chromaticity diagram. So we know that the sample d with indium concentration has white-light emission.

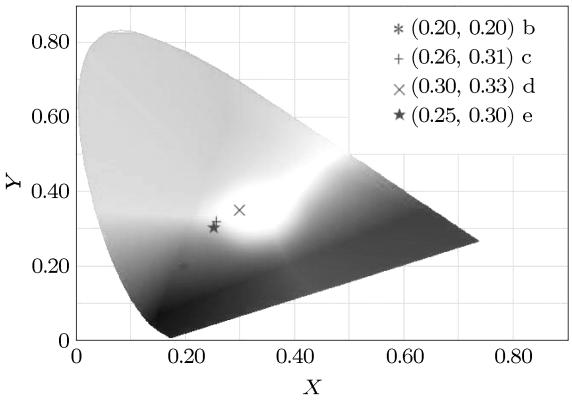


Fig. 5. Spectral chromaticity coordinates of samples a, b, c, d, and e.

Sample a possesses UV (ultra violet) emission at 380 nm and green emission at 530 nm. The UV emission is due to the band edge exciton complex.[17,18] People have different viewpoints on the mechanism of the green emission near 530 nm, but it is universally received that the point defects such as V_O, V_{Zn} (zinc vacancy), and Zn_i are responsible for the green emission.[19,20] Based on the previous study of the point defect energy level diagram,[21] we believe that green emission is due to the transition between V_O and V_{Zn}.[22] As shown in the spectra of samples b, c, d, and e, the UV emission peak is slightly redshifted, which is due to the fact that the amount of doped In exceeds the Mott critical density. According to the semiconductor–metal transition theory, when the impurity content is lower than the critical Mott density, the energy gap E_g increases; when the impurity content is higher than Mott critical density, the impurity incorporation can lead to the semiconductor energy gap E_g to be lowered, in other words, heavy doping reduces the band gap,[23,24] so the spectral red shift takes place. Beside the 535-nm peak caused by defects, there was a new peak appearing near 630 nm. This is due to the additional energy levels caused by the doped-In atoms. This new peak might be due to the transitions between these additional levels and the conduction band or valence band. We believe that the relative peak heights are due to the concentration of the generated V_O and the number of particle transitions between energy levels. In order to confirm that the dopant can generate a narrower band gap and additional energy levels, we use the first-principles method to calculate the energy band structure of ZnO (intrinsic and zinc completely replaced by indium). In the unit cell structure of the In-doped zinc model, the doping quantities of In are a series of fixed values. In order to comply with the result of XRD analysis, we constructed a $2\times1\times2$ ZnO supercell (including a total of 8 Zn atoms and 8 O atoms) and used an In atom to replace a Zn atom and the corresponding doping content is 12.5%. In the calculation, the valence electrons were in the O_2s, 2p states, In_5s, 5p states, and Zn_4s, 4p states, the Fermi level was taken as the zero energy reference point, and only the conduction band and valence band which was closest to Fermi level were considered. The calculated band structure is shown in Fig. 6. The band gap of undoped ZnO is 1.0 eV lower than the experimental value of 3.37 eV, which is caused by the introduction of generalized gradient approximation (GGA), a similar situation was also reported.[25,26]

The GGA or the local density approximation (LDA) will reduce the bandwidth. Since we only consider the relative width of the band gap, whether a new level is introduced and what the relative position of the introduced level is does not affect our analysis. It can be seen that after In is doped, the band gap becomes much narrower, much narrower than that of the intrinsic ZnO, and the Fermi level was included into the conduction band. The emergence of additional levels confirms our proposed interpretation of white light emission, the Fermi level is included into the conduction band, and the semiconductor possesses metal property, which proves that the doped ZnO has the characteristics of low resistivity.

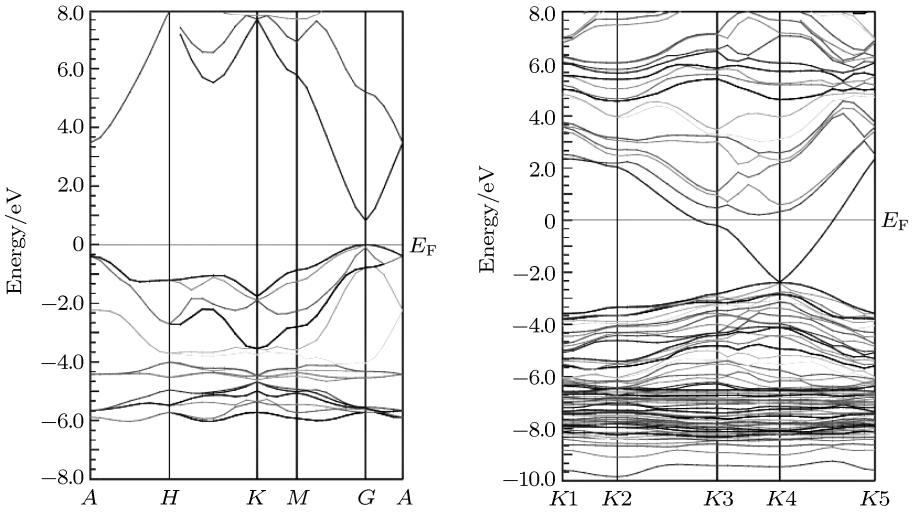


Fig. 6. Energy band diagrams of undoped and In-doped (12.5%) ZnO.

4. Conclusion

In is selected as the heavily doped element through sol–gel method. This can be used to control the resistivity and the emission spectrum of ZnO. Especially when the In content is 10%, white light emission can be observed. White light emission is due to the fact that the heavily doped In exceeds the critical Mott density, which leads energy gap E_g to decrease. The transition between V_O and V_{Zn} and the doped In caused transition between the additional doping level and the conduction band or valence band are also the reasons. The peak height of the white light is determined by the exciton number and the transition between different energy levels. These features of the ZnO provide important experimental and theoretical bases for the investigation and the development of a white light diode and new display technologies.

References

[1] Fan X M, Lian J S and Guo Z X 2005 *Appl. Surf. Sci.* **239** 176

[2] Zou J, Zhou S M and Xia C T 2005 *J. Crystal Growth.* **280** 185

[3] Huang J Z, Li S S and Feng X P 2010 *Acta Phys. Sin.* **59** 5839 (in Chinese)

[4] Zhou X, Wang S Q, Lian G J and Xiong G C 2006 *Chin. Phys.* **15** 199

[5] Liu Z W, Gu J F, Fu W J, Sun C W, Li Y and Zhang Q Y 2006 *Acta Phys. Sin.* **55** 5479 (in Chinese)

[6] Lu S C, Song G L, Xiao Z Y, Zhang J H and Huang S H 2002 *Chin. J. Lumin.* **23** 306 (in Chinese)

[7] Hao Y 2005 *Optoelectron. Technol. & Inform.* **18** 65 (in Chinese)

[8] Guo H H, Lin Z H, Feng Z F, Lin L L and Zhou J Z 2009 *J. Phys. Chem.* C **113** 12546

[9] Lin C F and Lee C Y http://nanotechweb.org/cws/article/tech/40848.html. 2009-10-30

[10] Guo C F, Ding X and Xu Y 2010 *J. Am. Ceram. Soc.* **93** 1708

[11] Zhang J M, Zhao D L and Shen Z M 2010 *High Perform. Ceram.* **6** 434

[12] Cao Y, Miao L and Tanemura S 2006 *J. Appl. Phys.* **45** 623

[13] Han M, Liu S and Meng L F 2009 *Chin. Hi-Tech Enterprises* **116** 54

[14] Cai W P and Guo J P 2009 *Metrology & Measurement Technique* **36** 39

[15] Chris G and Vande W 2001 *Physica* B **308** 310

[16] Pan Z W, Zu R D and Zhong L W 2001 *Science* **291** 1948

[17] Lyudmila N D, Lyudmila L T U and Yurn M J 2008 *Mater. Sci.* **43** 2143

[18] Lidia A, Gregorio B and Michele P J 2008 *Phys. Chem.* C **112** 4049

[19] Peng X P, Zang H and Wang Z G 2008 *Luminescence* **128** 328

[20] Yuan N Y, Fan L N and Li J H 2007 *Appl. Surf. Sci.* **253** 4990

[21] Li S S, Feng X P, Hang J J, Zhang Z and Tao Y Y 2010 *J. Funct. Mater.* **41** 113

[22] Fu Z X, Guo C X and Lin B X 1998 *Chin. Phys. Lett.* **15** 457

[23] Seung Y B, Hyun C C, Chan W N and Jeunghee P 2005 *Appl. Phys. Lett.* **86** 033102

[24] Jie J S, Wang G Z, Han X H, Yu Q X, Liao Y, Li G P and Hou J G 2004 *Chem. Phys. Lett.* **387** 466

[25] Nabi Z, Kellou A, Méçabih S, Khalfi A and Benosman N 2003 *Mater. Sci. Eng.* B **98** 104

[26] Xu J, Huang S P and Wang Z S 2009 *Solid State Commun.* **149** 527